반도체디스플레이기술학회지 제21권 제2호(2022년 6월)
Journal of the Semiconductor & Display Technology, Vol. 21, No. 2. June 2022.

Aerosol Deposition Nozzle Design for Uniform Flow Rate: Divergence Angle and Nozzle Length

Jae Young Kim[*,*], Young Jin Kim[**,***], Jeong Eun Jeon[*,***], Jun Woo Jeon[**,***], Beom Soo Choi[**,***], Jeong Won Choi[*,***] and Sang Jeen Hong[**,***†]**

[*]Department of Industrial and Management Engineering, Myongji University,
[**†]Department of Electronics Engineering, Myongji University,
[***]Semiconductor Equipment Engineering Program, Myongji University

ABSTRACT

Plasma density in semiconductor fabrication equipment becomes higher to achieve the improved the throughput of the process, but the increase of surface corrosion of the ceramic coated chamber wall has been observed by the increased plasma density. Plasma chamber wall coating with aerosol deposition prefer to be firm and uniform to prevent the potential creation of particle inside the chamber from the deformation of the coating materials, and the aerosol discharge nozzle is a good control factor for the deposited coating condition. In this paper, we investigated the design of the nozzle of the aerosol deposition to form a high-quality coating film. Computational fluid dynamics (CFD) study was employed to minimize boundary layer effect and shock wave. The degree of expansion, and design of simulation approach was applied to found out the relationship between the divergence angle and nozzle length as the key parameter for the nozzle design. We found that the trade-off tendency between divergence angle and nozzle length through simulation and quantitative analysis, and present the direction of nozzle design that can improve the uniformity of chamber wall coating.

Key Words : Chamber coating, Aerosol deposition, De Laval nozzle, Design of Simulation

1. Introduction

As the semiconductor fabrication process continues to become sensitive to minute change of the process environment, the reduction of particles in the plasma process chamber is considered to be a very important factor for the process yield. Currently, plasma etching equipment keeps increase the plasma density to achieve faster etch rate and higher process throughput by drastically increasing the applied RF power, and it also causes plasma chamber wall and chamber components are under attack from the high energy plasma, resulting in faster wear out of the components [1]. Plasma chamber wall is often dielectric coated to prevent the discharge of the generated charged particles of electrons and ions in the plasma, but the increased RF power also increases the chamber wall dielectric corrosion [2].

Ceramic has superior characteristics of the durability and less reaction with fluorine gas species in the plasma etching, and it has been actively employed as a plasma chamber wall coating materials in semiconductor industry [3,15]. Aerosol deposition of the ceramic powder is one of the most employed in coating industry because of the reduced substrate damage during the coating process [4,15], but the surface uniformity of the deposited coating materials is determined by the material characteristics, the robot arm control, and the aerosol discharge nozzle. It is reported that the surface morphology of the materials can be damaged by the plasma etch [1]. However, the improve of the surface morphology stands for the reaction of the morphology surface with plasma, and it becomes a serious problem of nonvolatile particle generation inside the plasma chamber.

Therefore, it is important to improve the surface morphology of the ceramic coating of the plasma process chamber to minimize a potential source of contaminant in current plasma etch environment.

High-density coating film deposition is possible by the collision of the submicron-sized raw ceramic powder with the constant high–speed, and the design of the material discharge nozzle, considering the boundary layer, and the shock wave, also plays a role for the quality of the aerosol deposition [5,15]. To improve the uniformity and surface morphology, it is required to design a nozzle structure capable of resulting the coating surface to be uniform and smooth on the surface. Uniform flow rate inside the nozzle reduces the degree of expansion, and a high-quality and uniform coating film can be achieved [6]. Divergence angle in nozzle design has been investigated to improve the discharge uniformity with the high maturity of research, and the effect of the nozzle length on the divergence angle also investigated in gas-blast erosion rig [7]. Therefore, we conducted a study with the divergence angle and nozzle length as the key variables of the aerosol deposition of ceramic coating for the plasma process chamber in this study. Several spray models were analyzed by CFD study using ANSYS to understand the fluid dynamics mechanism in size the nozzle considering the boundary conditions, and the design optimization to minimize the influence of the boundary layer inside the nozzle was performed employing a scheme of statistical design of simulation to improve the nozzle characteristics.

2. Experimental Theory

Aerosol deposition (AD) is a process in which sub micrometer-sized raw material powder can quickly collide with a substrate through a nozzle to form a high-density coating film. It is widely used to prevent damage to a semiconductor chamber and internal chamber parts by physical ion bombardment and chemical reaction with plasma. The equipment consists of a deposition chamber and an aerosol generator, is equipped with a vacuum pump to maintain tens of Torr, and functions to make an aerosol generator containing the deposition chamber and raw material powder a vacuum condition, as shown in Fig. 1 [4].

In the boundary layer, the velocity decreases due to the viscosity of the fluid on the surface where the fluid contacts the solid, resulting in a difference in velocity between the fluid passing through the side of the nozzle and the fluid passing through the center. Viscosity is a physical quantity indicating the degree of interference with motion, and the larger the distance, the greater the effect of viscosity [5]. Figure 2 presents the boundary layer effect in AD nozzle.

Shockwave effect is another important consideration that affects the flow of fluid. It is a shockwave caused by colliding with the substrate when the fluid is sprayed. Such a shock wave penetrates into the nozzle and hinder uniformity of flow. To minimize this effect, the nozzle outlet pressure and the chamber's internal pressure should be adjusted equally to achieve uniform flow and high-density coating [8].

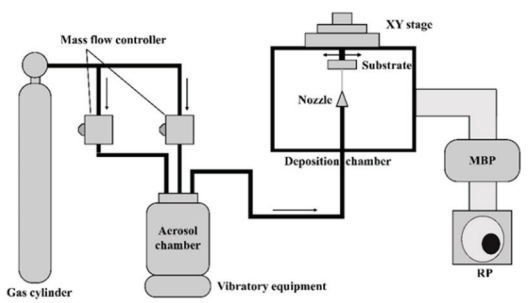

Fig. 1. Schematic aerosol deposition apparatus.

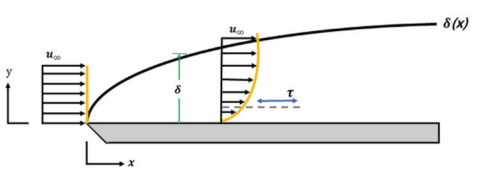

Fig. 2. Boundary Layer Effect, δ: boundary layer thickness, u_∞: free stream velocity value, ∞: free stream.

Since various plasma is used in the semiconductor process, materials with excellent plasma resistance should be used as equipment parts. For example, Aluminum oxide (Al_2O_3), yttrium oxide (Y_2O_3), yttrium oxyfluoride (YOF) are mainly used. Among them, Y-based materials have higher plasma resistance and deposition efficiency and fewer cracks or pores than existing oxide-based materials [4,9,13].

In aerosol deposition process, the nozzle requires a

convergent-divergent design, De Laval nozzle, in order to discharge the fluid in a supersonic speed with non-viscosity behavior. Fig. 3 shows three types of basic structures of De Laval nozzle. Among them, we chose the BLC nozzle which can minimize the boundary layer effect and the degree of expansion when the fluid discharged. It can be made by increasing the area ratio of AMNR nozzles to 7.0 [5,14].

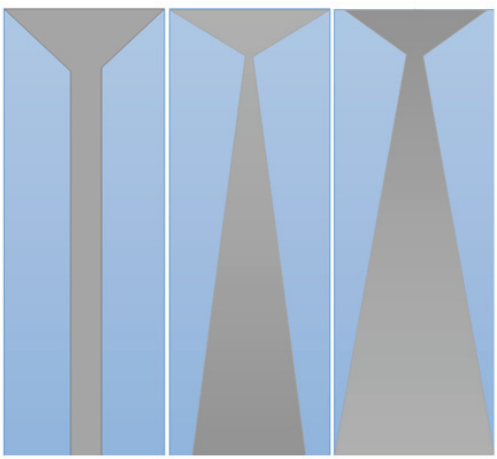

Fig. 3. Baseline nozzle, AMNR nozzle and BLC nozzle.

3. Experiment

We observed the trend of flow velocity uniformity relative to nozzle length, by using simulation and the result of discrete points of nozzle parameters in length and divergence angle can be received through image display with a computer.

3.1 Design Modeler & Mesh

We determined different divergence angle and nozzle geometries satisfying the minimum Boundary Layer effect requirements after the application of Design Modeler. Thus, nozzle for each different nozzle design is determined, Figs. 4 and 5 show the sample nozzle geometries.

First of all, we set $\left(\frac{A}{A^*}\right)$ = 1.688 which was derived by setting M = 2, γ = 1.4. Mach-number 2 is characterized by acting as a non-viscosity fluid in the Super-sonic area. Based on the experiments of the papers, they use nozzle design ranges between 1.4 - 2.5 to observe a tendency, therefore we

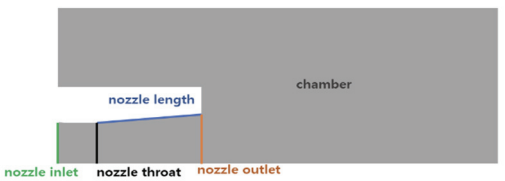

Fig. 4. Inside view of nozzle and chamber realized with Design Modeler.

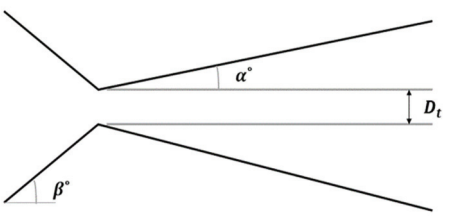

Fig. 5. Basic conical nozzle design (α = 2°-12°, β = 45°).

fixed 2 at their median.

$$\left(\frac{A}{A^*}\right)^2 = \frac{1}{M^2}\left[\frac{2}{\gamma+1}\left(1+\frac{\gamma-1}{2}M^2\right)\right]^{\frac{\gamma+1}{\gamma-1}} \quad (1)$$

Then, it is assumed that all the nozzle configurations have α = 2°~12° and β = 45°, and we confirmed that if the nozzle throat and nozzle exit area ratio is 7.0, it is helpful for the uniform flow rate of the nozzle. In case of all conditions are set the same, the area ratio is changed to 7.0, the radius of the nozzle exit is about 1.58 mm and the divergence angle is 9.3°. The speed was further improved, and the flow rate inside the nozzle was also uniform.

After design modeler process, we aimed for fine mesh, and set each line segment to same number of segments as the opposite line segment. we expected that it helps to reduce the time and effort required to obtain accurate results is produced.

3.2 Set up

We activated the Energy equation and the Realizable k-epsilon equation for turbulent flow [10]. First, the carrier gas minimizes to cause chemical reaction with other elements, therefore, we set 1.4 which is the ratio of specific heats of N_2. Then, through papers results, we set a value of 2666.45 Pa which is the pressure of the vacuum pressure for the gauge total pressure of the inlet and used 2719.778 the sum

of the operating condition value. Finally, we used 1 Torr (133.32 Pa) for the gauge total pressure of the outlet. [5, 10, 11].

As a result of implementation, the divergence angle was 3.174°. According to the paper on precautions for nozzle design, it was found that the divergence angle is the angle between 2° and 15° that does not impair the performance of the nozzle. In other words, it did not violate the law of divergence angle.

The nozzle length and divergence angle were set as variables affecting uniform flow formation and a total of four experiments were conducted. In particular, when we change the area ratio of the BLC nozzle to 7, the size of the divergence angle was set to a low divergence angle of 7° and a high divergence angle of 12° based on the central value of 8.6822. Since there is no numerical data available for reference regarding nozzle length, the lower-level length is arbitrarily set to 20 mm and the upper-level length is set to 50 mm.

4. Experimental Result

4.1 Simulation Analysis

When a nozzle is formed with a low-level divergence angle and length, the fluid cannot be sprayed at a high speed away from the nozzle outlet. In addition, it was confirmed that the degree of expansion was greater than the nozzle outlet area because it was not sufficiently accelerated inside the nozzle as shown in Fig 6 (a). When the nozzle is formed with a low-level divergence angle and a high length, the fluid is sprayed from the nozzle outlet to a long distance. In addition, it was confirmed that the degree of expansion was relatively small compared to the nozzle outlet area due to sufficient acceleration inside the nozzle in Fig. 6 (b).

In order to check the curvature through MINITAB, the divergence angle and nozzle length were set as intermediate values. When a nozzle is formed with a low-level divergence angle and length, the fluid is sprayed from the nozzle outlet to a long distance. In addition, it is sufficiently accelerated inside the nozzle, and the degree of expansion compared to the nozzle outlet area is relatively small as presented in Fig. 6 (c).

When the nozzle is formed with a low-level divergence angle and a high-level low length, the fluid is sprayed from the nozzle outlet to a long distance. In addition, it was confirmed that the degree of expansion was relatively small compared to the nozzle outlet area due to sufficient acceleration inside the nozzle in Fig. 6 (d). When the nozzle is formed with a high level of divergence angle and length, the fluid is not sprayed from the nozzle outlet in Fig. 6 (e).

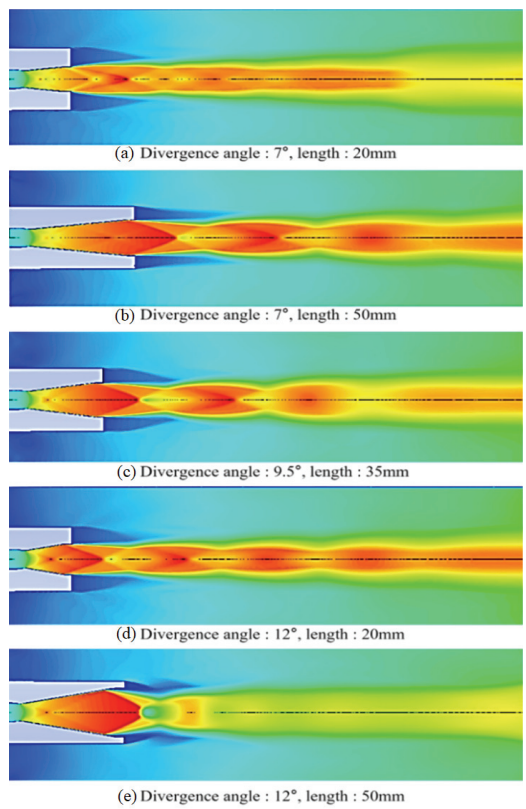

Fig. 6. Degree of nozzle injection according to variable.

4.2 Statistical Analysis

The work was conducted to statistically analyze the result values obtained through the shape of the nozzle implemented by ANSYS Fluent using MINITAB. Each factor A, B represents the number of nozzle length, divergence angle. In the case of a 2-factor 2-level complete factor experiment as shown in Table 1, the total number of experiments was very small with 4, so sufficient information was not obtained, so the experiment was repeated three times. In addition, a total of 15 experiments were conducted by adding three center points (nozzle length: 35mm / divergence angle of 9.5 degrees) between the two factors to determine whether there is a curvature between the two

Table 1. 2 factors, 2 levels experimental design

	A	B
Level 1	20 mm	7°
Level 2	50 mm	12°

Table 2. Simulation result

	Number of repetition	Average velocity	Velocity uniformity
7.0° 20 mm	300	902.7 ms^{-1}	0.8729
	500	953.7 ms^{-1}	0.8932
	700	1,049.9 ms^{-1}	0.9238
7.0° 50 mm	300	950.3 ms^{-1}	0.9115
	500	1,028.2 ms^{-1}	0.9460
	700	1,102.7 ms^{-1}	0.9770
12.0° 20 mm	300	925.3 ms^{-1}	0.9627
	500	986.4 ms^{-1}	0.9931
	700	1,082.7 ms^{-1}	0.9503
12.0° 50 mm	300	932.4 ms^{-1}	0.8457
	500	883.3 ms^{-1}	0.8411
	700	906.2 ms^{-1}	0.8489
9.5° 35 mm	300	976.3 ms^{-1}	0.8897
	500	1,043.9 ms^{-1}	0.9160
	700	1,109.5 ms^{-1}	0.9308

factors. While changing the two factors of the nozzle length (A) and the divergence angle (B), it was performed to check under what conditions a velocity uniformity (C) at two points of the nozzle was formed at a ratio of nearly 1.

Using the Eq. (2), the average speed and flow velocity uniformity were calculated and summarized as follows and summarized as shown in Table 2 [12].

$$\gamma = 1 - \frac{1}{2n}\sum_{i=1}^{n}\frac{\sqrt{(\omega_i - \overline{\omega})^2}}{\omega_i} \quad (2)$$

where ω_i= Local Velocity and $\overline{\omega}$ = Average Velocity.

When the null hypothesis is set to "no curvature effect" and the alternative hypothesis to " curvature effect exists", the curvature analysis results from the ANOVA table show that the null hypothesis can be adopted because the *p*-value of center point is greater than 0.05 in Table 3.

Table 3. Estimated Effects and Coefficients for Velocity uniformity

	Coef.	SE Coef.	T	P
Cons.	0.91385	0.006663	137.15	0.000
A	-0.01882	0.006663	-2.82	0.018
B	-0.00688	0.006663	-1.03	0.326
A*B	-0.04292	0.006663	-6.44	0.000
Ct Pt	-0.00168	0.014899	-0.11	0.912

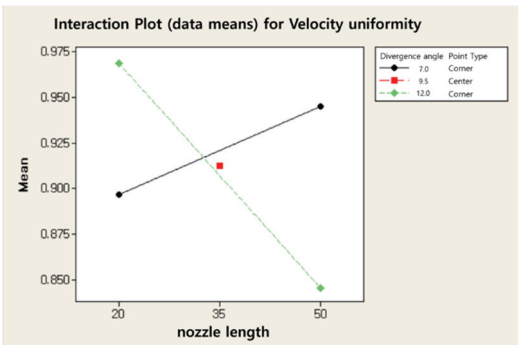

Fig. 7. Interaction Plot for Velocity uniformity.

Figure 7 can also confirm the curvature effect, and the curvature effect cannot be considered to exist because the red dot is not far from the black straight line. Through the regression equation obtained based on the results of the full factor experiment without curvature effect, a response optimization analysis was conducted to find out where the velocity uniformity in the nozzle was close to 1. As a result of the response optimization analysis as shown in Table 4, it was found that the flow rate ratio of the two points in the nozzle was 0.9687 at the lower right vertex of the rectangle (nozzle length: 20mm / divergence angle: 12 degrees).

Table 4. Response optimization analysis result

	Divergence angle	Nozzle length
Optimal Hi	12.0	50.0
D Cur	12.0	20.0
0.80302 Lo	7.0	20.0
Target : 1.0 $y = 0.9687$ $d = 0.80302$	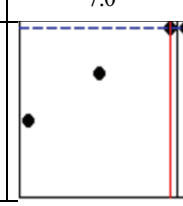	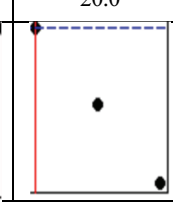

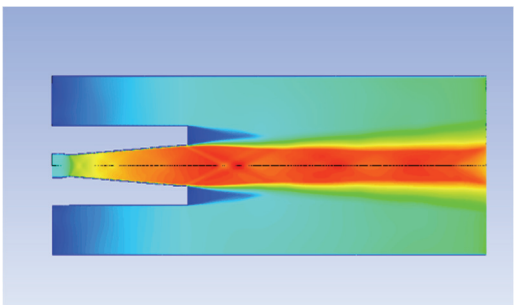

Fig. 8. Simulation result of nozzle (nozzle length: 70 mm, divergence angle: 4 degrees).

Table 5. Simulation result

	Average velocity	Velocity uniformity
4.0° 70mm	1061.32 ms^{-1}	0.9810

Additionally, in the velocity uniformity analysis, within our simulation range, 12 degrees at 20 mm was the best result as shown in Fig. 8, followed by 7 degrees at 50 mm. Based on this result, it could be inferred that there is a tendency of trade-off between the nozzle length and the divergence angle. We conducted a wider range of experiments to confirm the trade-off relationship. As a result, when the divergence angle was 4 degrees and the nozzle length was 70 mm, the best value for speed uniformity was obtained as presented in Table 5, and it was confirmed that there is a trade-off tendency between the nozzle length and the divergence angle.

5. Conclusion

In this paper, internal flow simulation analysis of nozzles with different divergence angles and nozzle lengths is performed. Using the program (including ANSYS Fluent, MINITAB), we analyzed the nozzle structure that could minimize the degree of expansion relative to the nozzle outlet area by focusing on the flow of the nozzle internal flow. This is to create a uniform flow rate, and we found a relationship between the degree of expansion and the uniform flow rate. The simulation results of inlet pressure and outlet pressure set as parameters were visually compared under the same conditions, and finally, a numerical optimized value for a nozzle structure capable of forming a uniform flow rate inside a nozzle was derived. From these results, it can be expected that the improved nozzle structure can minimize the effect of the boundary layer and shockwave, create a uniform flow rate, and increase the efficiency for coating compared to the existing nozzle.

Summarized, the advantages of improved nozzle structure can form a high quality and density coating film on a linear in the aerosol deposition process. This will increase chamber life and form a consistent process atmosphere, which will eventually have a positive effect on yield. And we hope that the trade-off tendency analysis between the nozzle length and the divergence angle we have proven will contribute to the development of nozzle research in the future.

Acknowledgement

This work was supported by Korea Institute for Advancement of Technology (KIAT) grant funded by the Korea Government (MOTIE). (P0008458, The Competency Development Program for Industry Specialist.)

References

1. S. J. Fonash, “An Overview of Dry Etching Damage and Contamination Effects”, *Journal of The Electrochemical Society*, Vol. 137, No. 12, pp. 3885-3886, 1990.
2. N. Ito, T. Moria, F. Uesugi, M. Matsumoto, S. Liu, and Y. Kitayama, “Reduction of Particle Contamination in Plasma-Etching Equipment by Dehydration of Chamber Wall”, *Japanese Journal of Applied Physics*, Vol. 47, No. 5, pp. 3630–3634, 2008.
3. E. Bakan, R. Vaben, “Ceramic Top Coats of Plasma-Sprayed Thermal Barrier Coatings: Materials, Processes, and Properties”, *J Therm. Spray Tech*, pp. 1-73, 2017.
4. H. Ashizawa, K. Masakatsu, and K. Yoshida, “Micro–structure and Plasma Corrosion Behavior of Yttria Coatings Prepared by The Aerosol Deposition Method”, *Journal of the American Ceramic Society*, Vol. 103, No. 12, pp. 7031-7040, 2020.
5. T. L. Hoffman, “Nozzle Design for Vacuum Aerosol Deposition of Nanostructured Coatings”, *Ph.M. dissertation, Dept. Elect. Eng.*, Arizona State Univ., 2017.
6. C. Li, N. Singh, A. Andrews, B. A. Olson, T. E. Schwartzentruber, and C. J. Hogan Jr, “Mass, Momentum, and Energy Transfer in Supersonic Aerosol Deposition Processes”, *International Journal of Heat and Mass Transfer*, Vol. 129, pp 1161-1171, 2019.

7. J. Singh, L. E. Zerpa, Benjamin Partington, and Jose Gamboa, “Effect of Nozzle Geometry on Critical-Subcritical Flow Transitions”, *Heliyon*, pp 1-19, 2019.
8. J. J. Park, M. W. Lee, S. S. Yoon, H.Y. Kim, S. C. James, S. D. Heister, S. Chandra, W.H. Yoon, D.S Park, and J. Ryu, “Supersonic Nozzle Flow Simulations for Particle Coating Applications: Effects of Shockwaves, Nozzle Geometry, Ambient Pressure, and Substrate Location upon Flow Characteristics”, *Journal of Thermal Spray Technology*, Vol. 20, No. 3, pp. 514-522, 2011.
9. K.B Kim, D. Kim, J. Lee, Y.S. Oh, H.T. Kim, H. Kim, and S.M. Lee, “Erosion Behavior of YAG Ceramics Under Fluorine Plasma and their XPS Analysis”, *Journal of the Korean Ceramic Society*, Vol. 46, No. 5, pp. 456-461, 2009.
10. N.D. Deshpande, S. S. Vidwans, P R. Mahale, R. Joshi, and K.R. Jagtab, “Theorical & CFD Analysis of De Laval Nozzle”, *International Journal of Mechanical and Production Engineering 2*, pp. 33-36, 2014.
11. M.W. Lee, J.J. Park, D.Y. Kim, S.S. Yoon, H.Y. Kim, D.H. Kim, S.C. James, S. Chandra, Thomas Coyle, J.H. Ryu, W.H. Yoon and D.S. Park, “Optimization of Supersonic Nozzle Flow for Titanium Dioxide Thin-Film Coating by Aerosol Deposition”, *Journal of Aerosol Science*, Vol. 42, Issue 11, pp. 771-780, 2011.
12. Y. Kim, D. Han, and Y. Baek, “A Study on the Flow Uniformity and Characteristics of Exhaust gas in Diesel Particulate Filter/Diesel Oxidation Catalyst of Ship Diesel Reduction System by Computational Fluid Dynamics”, *Clean Technol*., Vol. 25, No. 2, pp. 153-160, 2019.
13. D. Hanft, J. Exner, M. Schubert, T. Stöcker, P. Fuierer and R. Moos, "An Overview of the Aerosol Deposition Method: Process Fundamentals and New Trends in Materials Applications," *Journal of Ceramic Science and Technology*, Vol. 6, No. 3, pp. 147-182, 2015.
14. Yesu Ratnam.Maddu, Shaik. Saidulu, Md. Azeem & S. Jabiulla, “Design and Fluid Flow Analysis of Convergent-Divergent Nozzle”, *International Journal of Engineering Technology Science and Research (IJETSR)*, Vol. 5, No. 4, pp. 903-909, 2018.
15. Nazarenus T, Schlesier K, Biberger S, Exner J, Kita J, Köhler A, “Post-treatment of powder aerosol deposited oxide ceramic films by high power LED”, *Journal of the American Ceramic Society*, pp. 1540-1553, 2022.

접수일: 2022년 5월 24일, 심사일: 2022년 6월 20일, 게재확정일: 2022년 6월 22일